Treatment Monitoring of Immunotherapy and Targeted Therapy Using ^{18}F-FET PET in Patients with Melanoma and Lung Cancer Brain Metastases: Initial Experiences

Norbert Galldiks[1–3], Diana S.Y. Abdulla[2,4], Matthias Scheffler[2,4], Fabian Wolpert[5], Jan-Michael Werner[1], Martin Hüllner[6], Gabriele Stoffels[3], Viola Schweinsberg[2,7], Max Schlaak[2,7], Nicole Kreuzberg[2,7], Jennifer Landsberg[2,8], Philipp Lohmann[3,9], Garry Ceccon[1], Christian Baues[2,10], Maike Trommer[2,10], Eren Celik[2,9], Maximilian I. Ruge[2,9], Martin Kocher[3,9], Simone Marnitz[2,10], Gereon R. Fink[1,3], Jörg-Christian Tonn[11], Michael Weller[5], Karl-Josef Langen[3,12], Jürgen Wolf[2,4], and Cornelia Mauch[2,7]

[1]Department of Neurology, Faculty of Medicine and University Hospital Cologne, University of Cologne, Cologne, Germany; [2]Center of Integrated Oncology, Universities of Aachen, Bonn, Cologne, and Duesseldorf, Germany; [3]Institute of Neuroscience and Medicine (INM-3, -4), Research Center Juelich, Juelich, Germany; [4]Lung Cancer Group, Department I of Internal Medicine, Faculty of Medicine and University Hospital Cologne, University of Cologne, Cologne, Germany; [5]Department of Neurology and Brain Tumor Center, University Hospital and University of Zurich, Zurich, Switzerland; [6]Department of Nuclear Medicine, University Hospital and University of Zurich, Zurich, Switzerland; [7]Department of Dermatology, Faculty of Medicine and University Hospital Cologne, University of Cologne, Cologne, Germany; [8]Department of Dermatology, University Hospital Bonn, Bonn, Germany; [9]Department of Stereotaxy and Functional Neurosurgery, Faculty of Medicine and University Hospital Cologne, University of Cologne, Cologne, Germany; [10]Department of Radiation Oncology, Faculty of Medicine and University Hospital Cologne, University of Cologne, Cologne, Germany; [11]Department of Neurosurgery, University Hospital LMU Munich, Munich, Germany; and [12]Department of Nuclear Medicine, RWTH University Hospital Aachen, Aachen, Germany

We investigated the value of *O*-(2-^{18}F-fluoroethyl)-L-tyrosine (^{18}F-FET) PET for treatment monitoring of immune checkpoint inhibition (ICI) or targeted therapy (TT) alone or in combination with radiotherapy in patients with brain metastasis (BM) since contrast-enhanced MRI often remains inconclusive. **Methods:** We retrospectively identified 40 patients with 107 BMs secondary to melanoma (n = 29 with 75 BMs) or non–small cell lung cancer (n = 11 with 32 BMs) treated with ICI or TT who had ^{18}F-FET PET (n = 60 scans) for treatment monitoring from 2015 to 2019. Most patients (n = 37; 92.5%) had radiotherapy during the course of the disease. In 27 patients, ^{18}F-FET PET was used to differentiate treatment-related changes from BM relapse after ICI or TT. In 13 patients, ^{18}F-FET PET was performed for response assessment to ICI or TT using baseline and follow-up scans (median time between scans, 4.2 mo). In all lesions, static and dynamic ^{18}F-FET PET parameters were obtained (i.e., mean tumor-to-brain ratios [TBR], time-to-peak values). Diagnostic accuracies of PET parameters were evaluated by receiver-operating-characteristic analyses using the clinical follow-up or neuropathologic findings as a reference. **Results:** A TBR threshold of 1.95 differentiated BM relapse from treatment-related changes with an accuracy of 85% (P = 0.003). Metabolic responders to ICI or TT on ^{18}F-FET PET had a significantly longer stable follow-up (threshold of TBR reduction relative to baseline, ≥10%; accuracy, 82%; P = 0.004). Furthermore, at follow-up, time to peak in metabolic responders increased significantly (P = 0.019). **Conclusion:** ^{18}F-FET PET may add valuable information for treatment monitoring in BM patients treated with ICI or TT.

Received Apr. 27, 2020; revision accepted Jul. 30, 2020.
For correspondence or reprints contact: Norbert Galldiks, University of Cologne, Kerpener Strasse 62, Cologne 50937, Germany.
E-mail: norbert.galldiks@uk-koeln.de
Published online Sep. 4, 2020.

Key Words: checkpoint inhibitors; pseudoprogression; response assessment; treatment-related changes; radionecrosis

J Nucl Med 2021; 62:464–470
DOI: 10.2967/jnumed.120.248278

Brain metastasis (BM) develops in 20%–40% of patients with late-stage cancer and is associated with a poor prognosis. Frequently used treatment options are radiosurgery, whole-brain radiation therapy, surgical resection in oligometastases, and systemic cytotoxic chemotherapy (*1*). The advent of immunotherapy using immune checkpoint inhibition (ICI) and targeted therapy (TT) has considerably improved the overall survival of cancer, particularly in patients with melanoma or lung cancer (*2–4*). Additionally, more recent trials have shown that patients with BM from melanoma or lung cancer may also benefit from these agents alone or in combination (*5–8*).

After various newer treatment options for patients with BM such as immunotherapy using ICI or TT, imaging findings on contrast-enhanced anatomic MRI can be highly variable, especially when these agents are used in combination with radiotherapy, and the interpretation regarding the differentiation of treatment-related changes from BM relapse is often difficult (*9*). Additionally, this uncertainty may also negatively affect the assessment of response to these newer treatment options, particularly if applied in combination (e.g., ICI or TT plus radiotherapy) (*10*). For example, immunogenic reactions related to ICI may trigger inflammation and intratumoral infiltrates, including cytotoxic T cells, thereby leading to MRI findings that suggest BM relapse. Correspondingly, histopathology typically shows inflammatory cells (*11*) but not mitotically active tumor cells. This problem is also aggravated by the fact that progressive

imaging changes on anatomic MRI early after treatment initiation might represent an actual tumor progression that ultimately becomes controlled by a delayed immune response (*9*). Although the Immunotherapy Response Assessment in Neuro-Oncology (iRANO) Working Group recommended both clinical and standard MRI criteria to overcome the clinical problem of immunotherapy-related pseudoprogression (*9*), these newer treatment options seem to impose demands on brain imaging beyond those offered by routine anatomic MRI techniques.

Metabolic PET imaging may help to overcome some of these imaging challenges. Radiolabeled amino acids are of particular interest for brain tumor imaging using PET because of their increased uptake in neoplastic tissue but low uptake in normal brain parenchyma, resulting in an improved tumor-to-brain contrast compared with glucose PET (*12*). Importantly, a key feature of amino acid tracers is their ability to pass the intact blood–brain barrier, allowing depiction of tumor tissue beyond contrast enhancement in MRI (*12*). Increased uptake of radiolabeled amino acids is related to amino acid transporters of the L-type, which are often overexpressed in brain tumors (*13,14*). L-type transporter overexpression in BM makes intracranial metastases also a compelling target for amino acid PET imaging (*15*). Moreover, the iRANO group has analyzed the additional diagnostic value of amino acid PET in patients with glioma and BM and recommended the use of this imaging technique in addition to conventional MRI, especially for delineation of brain tumor extent, assessment of treatment response, and differentiation of treatment-related changes from tumor progression (*16–18*).

However, only few data are currently available for the evaluation of ICI- or TT-treated BM patients in combination without or with radiotherapy using amino acid PET. The purpose of the present study was to investigate the value of amino acid PET using *O*-(2-^{18}F-fluoroethyl)-L-tyrosine (^{18}F-FET) as an additional imaging method, compared with conventional contrast-enhanced MRI alone, for treatment monitoring in predominantly heavily pretreated patients with BM from melanoma or non–small cell lung cancer (NSCLC) treated with ICI or TT alone or in combination with radiotherapy.

MATERIALS AND METHODS

Patients

From 2015 to 2019, 40 adult patients with metastatic brain tumors secondary to histomolecularly defined malignant melanoma (MM; $n = 29$) or NSCLC ($n = 11$) (mean age, 59 ± 13 y; range, 27–83 y; 8 women and 32 men) treated with ICI or TT who underwent in total 60 ^{18}F-FET PET scans for treatment monitoring were included in this retrospective study. All patients had at least 1 contrast-enhancing lesion ($n = 75$ in MM patients and $n = 32$ in NSCLC patients; total number of contrast-enhancing lesions, 107) on cerebral MRI. Most patients ($n = 37$; 92.5%) had radiotherapy during the course of disease (Supplemental Tables 1–3; supplemental materials are available at http://jnm.snmjournals.org).

Twenty-seven of these 40 patients with equivocal MRI findings after ICI, TT, radiotherapy, or combinations thereof were referred to the Research Center Juelich ($n = 18$) or to the Brain Tumor Center of the University Hospital Zurich ($n = 9$) to differentiate actual BM relapse from treatment-related changes using ^{18}F-FET PET (total number of ^{18}F-FET PET examinations, 32). A detailed overview of the patients' pretreatment is listed in Supplemental Tables 1 and 2.

The remaining 13 patients were referred to the Research Center Juelich for evaluation of the treatment effects after ICI, TT, radiotherapy, or combinations thereof using ^{18}F-FET PET. In contrast to the other 27 patients, each of these patients had a baseline scan and at least 1 follow-up scan (range, 1–2 scans) (median time between baseline and first follow-up scan, 4.2 mo; total number of scans, 28). The applied therapy, including the pretreatment before ^{18}F-FET PET imaging, is listed in Supplemental Table 3.

The local ethics committees approved the retrospective analysis of the data. There was no conflict with the Declaration of Helsinki. All subjects had given written informed consent for the PET investigation.

Conventional MRI

In accordance with the International Standardized Brain Tumor Imaging Protocol (*19*), MRI was performed using a 1.5- or 3.0-T MRI scanner with a standard head coil before and after administration of a gadolinium-based contrast agent (0.1 mmol/kg of body weight). The sequence protocol comprised at least 3-dimensional isovoxel T1-weighted, 2-dimensional T2-weighted, and 2-dimensional fluid-attenuated inversion recovery-weighted sequences. MRI changes at first follow-up, compared with the baseline scan, were assigned according to the iRANO criteria for BM (*20*).

Diagnosis of Treatment-Related Changes and Evaluation of Treatment Response

In 2 cases, tissue was available and treatment-related changes were diagnosed by prominent necrosis with no or only minimal identifiable tumor remnants in 1 case and the presence of viable tumor tissue confirming BM relapse in the other case.

In the remaining patients, a neuropathologic diagnosis was unavailable, and iRANO criteria (*9*) were considered for diagnostic assessment. According to the iRANO criteria (*9*), treatment-related changes were assumed under 3 conditions: the lesions showed spontaneous shrinkage or remained stable in size on contrast-enhanced MRI during a follow-up of at least of 3 mo (median follow-up, 7 mo; range, 3–25 mo); the clinical condition remained stable; and no new neurologic symptoms occurred or neurologic deficits remained unchanged.

Response to the applied treatment on ^{18}F-FET PET was considered if a decrease in metabolic activity at follow-up was associated with a stable clinical course for at least 6 mo; that is, the clinical condition remained stable or even improved and no new neurologic symptoms occurred, or existing neurologic deficits remained unchanged, as documented in the patients' charts.

^{18}F-FET PET Imaging

The amino acid ^{18}F-FET was produced via nucleophilic ^{18}F-fluorination with a radiochemical purity of greater than 98%, specific radioactivity greater than 200 GBq/μmol, and a radiochemical yield of about 60% (*21*). According to international guidelines for brain tumor imaging using labeled amino acid analogs (*18*), patients fasted for at least 4 h before the PET measurements.

At the Research Center Juelich, all patients underwent a dynamic PET scan from 0 to 50 min after injection of 3 MBq of ^{18}F-FET per kilogram of body weight. PET imaging was performed either on an ECAT Exact HR+ PET scanner in 3-dimensional mode ($n = 19$ patients; axial field of view, 15.5 cm; Siemens) or simultaneously with 3.0-T MRI using a BrainPET insert ($n = 12$ patients; axial field of view, 19.2 cm; Siemens). The BrainPET is a compact cylinder that fits into the bore of the Magnetom Trio MR scanner (*22*). Iterative reconstruction parameters were 16 subsets and 6 iterations using the ordered-subsets expectation maximization algorithm for the ECAT HR+ PET scanner or 2 subsets and 32 iterations using the ordinary-Poisson ordered-subsets expectation maximization algorithm for the BrainPET. Data were corrected for randoms, scattered coincidences, dead time, and motion, for both systems. Attenuation correction was based on a transmission scan for the ECAT HR+ PET scan and on a template-based

approach for the BrainPET scan (*22*). The reconstructed dynamic datasets consisted of 16 time frames (5 × 1, 5 × 3, and 6 × 5 min) for both scanners.

At the University Hospital Zurich, ^{18}F-FET PET images were acquired on a PET/CT scanner (Discovery 690 standard; GE Healthcare; $n = 4$ patients) or on a PET/MR (3.0-T) scanner (Signa PET/MR; GE Healthcare; $n = 5$ patients). The patients were injected with a standardized dose of 130 MBq 20 min before (PET/CT) or immediately before (PET/MR) the dynamic PET acquisition. All PET images were reconstructed using the ordered-subsets expectation maximization algorithm in conjunction with point-spread-function modeling. The reconstructed dynamic datasets consisted of 8 time frames (8 × 5 min) for the PET/MR scanner and 4 time frames (4 × 5 min) for the PET/CT scanner.

^{18}F-FET PET Data Analysis

^{18}F-FET uptake in the tissue was expressed as SUV by dividing the radioactivity (kBq/mL) in the tissue by the radioactivity injected per gram of body weight. All PET and MR images were coregistered, and the fusion results were inspected and, if necessary, adapted on the basis of anatomic landmarks. For evaluation of the ^{18}F-FET data, summed PET images over 20–40 min after injection were used. Mean tumoral ^{18}F-FET uptake was determined by a 2-dimensional autocontouring process using a tumor-to-brain ratio (TBR) at a threshold of 1.6 (*18,23,24*). Mean TBR (TBR_{mean}) was calculated by dividing the SUV_{mean} of the tumor region of interest (ROI) by the SUV_{mean} of a larger reference ROI placed in the semioval center of the contralateral unaffected hemisphere including white and gray matter (*18,24,25*). In the case of multiple BMs, ROI analyses for TBR_{mean} calculation were performed for each metastasis separately. Because of the use of different PET scanners ($n = 4$) in 2 centers, calculations of maximum TBR (TBR_{max}) were not obtained, because TBR_{max} may vary considerably (*26*) and the comparability may be affected by the different spatial resolution of the PET scanners.

At the Research Center Juelich, time–activity curves for ^{18}F-FET uptake (SUV_{mean}) in the tumor were generated by application of a spheric volume of interest with a volume of 2 mL centered on the voxel with the maximum tumor uptake (*27*) and the reference ROI as described above for the entire dynamic dataset. A reference time–activity curve was generated by placing a reference ROI in the unaffected brain tissue as reported previously (*27*). For time–activity curve evaluation, the time to peak (TTP; time in minutes from the beginning of the dynamic acquisition up to the SUV_{max} of the lesion) was determined. Because of the different dynamic ^{18}F-FET PET acquisition protocol used in the 9 patients from the University Hospital Zurich, a time–activity curve evaluation by TTPs in these 9 patients was not performed.

Statistical Analyses

Descriptive statistics are provided as mean and SD or median and range. The Student *t* test was used to compare 2 groups. The Mann–Whitney rank-sum test was used when variables were not normally distributed. The change in TTPs in the same patients were compared using the paired *t* test.

The diagnostic performance of TBR_{mean} for differentiation of BM relapse from treatment-related changes was assessed by receiver-operating-characteristic (ROC) curve analyses, using histologic confirmation or the clinical course as a reference. In the case of multiple BMs, the lesion with the highest metabolic activity was selected for the ROC analysis.

To determine the optimal threshold of TBR_{mean} for identifying responders to ICI, TT, radiotherapy, or combinations thereof, an ROC analysis was calculated using a stable clinical course of 6 mo as a reference. The lesion with the highest metabolic activity was selected for response assessment—that is, relative TBR_{mean} changes during follow-up relative to baseline. Furthermore, the lesion with the highest metabolic activity was selected for TTP calculation.

As a measure of the test's diagnostic quality, the area under the ROC curve (AUC), its SE, and its level of significance were determined. The decision cutoff was considered optimal when the product of paired values for sensitivity and specificity reached its maximum. The diagnostic performance of TBR_{mean} in combination with the corresponding TTP was evaluated by the Fisher exact test for 2 × 2 contingency tables.

P values of 0.05 or less were considered significant. Statistical analyses were performed using SPSS statistics (release 26.0, SPSS Inc.).

RESULTS

TT and ICI Therapy in Relation to Radiotherapy

Most patients ($n = 37$; 92.5%) had radiotherapy during the course of the disease. Before ^{18}F-FET PET imaging, 70% of the patients ($n = 28$) had undergone radiotherapy, either as a single modality (35%; $n = 14$) or in combination with ICI or TT (35%; $n = 14$). Radiosurgery was the most frequently used radiotherapy modality (60%; range of surface radiation dose, 16–25 Gy/50%–80% isodose level) (Supplemental Table 1).

Diagnosis of Recurrent BM and Treatment-Related Changes

After multimodal treatment including radiotherapy, ICI, TT, and combinations thereof (Supplemental Tables 1 and 2), a treatment-related change was diagnosed in 17 patients. This was based on stable neurologic symptoms and no significant enlargement of the lesion on further follow-up MR images after a median of 7 mo (range, 3–25 mo) in 16 patients, or on neuropathology in 1 patient. In total, recurrent BMs were diagnosed in 10 patients. Based on the deterioration of the clinical condition (i.e., reduction of the Karnofsky performance index < 60%, progression or development of new neurologic symptoms, or subsequent cancer-related death), as well as progression in size on contrast-enhanced MRI during follow-up (median follow-up time, 3 mo; range, 2–5 mo), recurrent BMs were diagnosed in 9 patients. In 1 patient, BM recurrence was diagnosed neuropathologically.

Comparison of Static and Dynamic ^{18}F-FET PET Parameters in Recurrent BM and Treatment-Related Changes

TBR_{mean} was significantly higher in patients with BM relapse ($n = 10$) than in patients with treatment-related changes ($n = 17$) (2.4 ± 0.8 vs. 1.7 ± 0.3, $P < 0.001$) (Fig. 1). In contrast, TTP was not significantly different between patients with BM relapse and treatment-related changes (27.7 ± 15.3 min vs. 34.5 ± 5.0 min, $P = 0.206$). The TBR_{mean} and TTP for each patient are listed in Supplemental Table 4.

Diagnostic Performance of TBR_{mean} and TTP

The ROC analysis revealed that the diagnostic accuracy of TBR_{mean} for the correct identification of recurrent BM reached 85% (AUC, 0.85 ± 0.09; sensitivity, 70%; specificity, 94%; cutoff, 1.95; $P = 0.003$). In contrast, the ROC analysis of the dynamic ^{18}F-FET PET parameter TTP yielded a lower diagnostic performance for the correct identification of recurrent BM (AUC, 0.61 ± 0.18; sensitivity, 100%; specificity, 57%; cutoff, 27.5 min; $P = 0.464$). For the diagnosis of BM relapse, the presence of a TBR_{mean} of more than 1.95 in combination with a TTP of less than 27.5 min did not further increase the diagnostic performance (accuracy, 82%; sensitivity, 57%; specificity, 100%; $P = 0.015$).

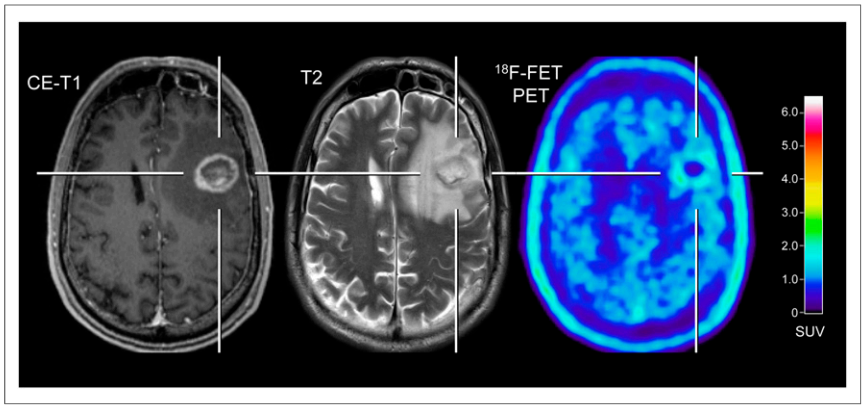

FIGURE 1. Patient with melanoma BM pretreated with radiosurgery concurrent with nivolumab, and dabrafenib in combination with trametinib (patient 9; Supplemental Tables 2 and 4). In contrast to progressive MRI, amino acid PET using ^{18}F-FET shows no significant uptake and is consistent with treatment-related changes. After PET imaging, survival time was 24 mo. CE = contrast-enhanced.

Assessment of Treatment Response

In 13 patients, ^{18}F-FET PET was performed for the assessment of response to a treatment regimen including ICI or TT using baseline and follow-up ^{18}F-FET PET scans (median time between scans, 4.2 mo). Nine of these 13 patients (69%) had ICI or a TT concurrent with radiotherapy (applied within the first 4 wk after radiotherapy initiation). A detailed overview on the pretreatment and the applied treatment is shown in Supplemental Table 3.

ROC analysis revealed that at follow-up a relative reduction in TBR_{mean} of 10% or more separated metabolic ^{18}F-FET PET responders (n = 6) with a stable clinical course of at least 6 mo or more (median follow-up time, 10.5 mo; range, 6–18 mo) from nonresponders with a stable clinical course of less than 6 mo (n = 5; median follow-up time, 4 mo; range, 2–5 mo) with a sensitivity of 80%, a specificity of 83%, and an accuracy of 82% (AUC, 0.78 ± 0.12; P = 0.121). Two of 13 patients examined for the evaluation of treatment response using ^{18}F-FET PET had to be excluded from ROC analysis (loss to follow-up in 1 patient, death related to causes other than cancer in the other patient). Additionally, metabolic responders on ^{18}F-FET PET (relative reduction of TBR_{mean}, ≥10%) had a significantly longer stable clinical course than nonresponding patients (median time, 10.5 vs. 4 mo; P = 0.004).

Furthermore, in metabolic ^{18}F-FET PET responders, TTP at follow-up increased significantly relative to the baseline TTP (22.0 ± 9.7 min vs. 36.7 ± 5.2 min, P = 0.019). In contrast, ^{18}F-FET PET metabolic nonresponders showed at follow-up a significant decrease in TTP (23.0 ± 11.0 min vs. 3.4 ± 1.3 min, P = 0.013). The TBR_{mean} and TTP for each patient are listed in Supplemental Table 5.

^{18}F-FET PET Findings of Metabolic Responders and Nonresponders in Relation to MRI

In 4 of 13 patients (31%), ^{18}F-FET PET findings at follow-up were discrepant with the changes on contrast-enhanced MRI (Supplemental Table 3). In these cases, ^{18}F-FET PET provided additional information for treatment response evaluation beyond the information provided by contrast-enhanced MRI alone. In particular, ^{18}F-FET PET in 2 metabolic responders (patients 1 and 8; Supplemental Tables 3 and 5) showed a significant decrease in metabolic activity (TBR_{mean}, −28% and −15%, respectively), although MRI changes were consistent with progression according to iRANO criteria (Fig. 2). Furthermore, in contrast to a patient (patient 3; Supplemental Tables 3 and 5) with unchanged MRI (stable disease according to iRANO criteria) at follow-up, the ^{18}F-FET PET indicated a metabolic response with a significant decline in TBR_{mean} (−19%). Moreover, although 1 patient had lesions with increasing metabolic activity (metabolic nonresponder; TBR_{mean} increase, 10%), the corresponding MRI suggested even a partial response according to iRANO criteria (patient 9; Supplemental Tables 3 and 5; Fig. 3).

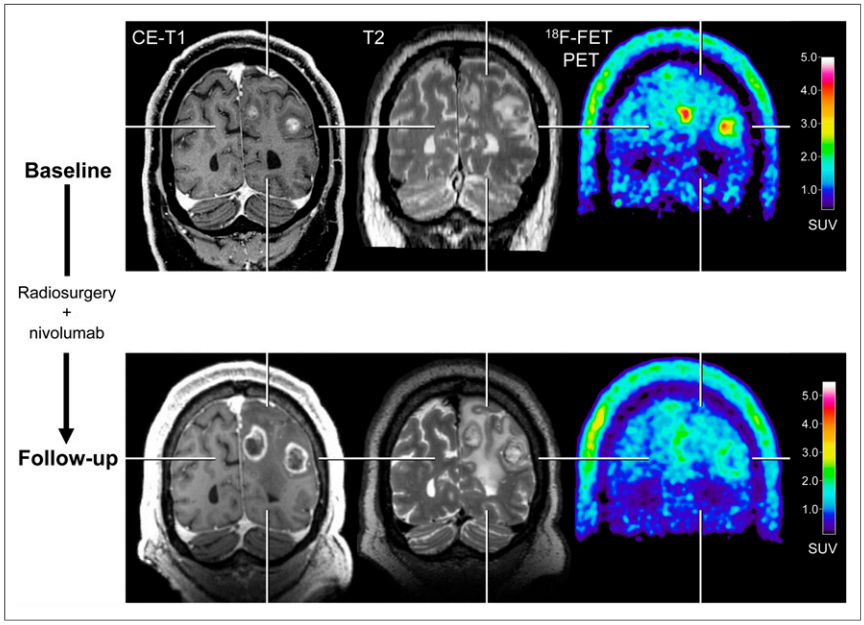

FIGURE 2. After radiosurgery concurrent with nivolumab in 59-y-old patient with melanoma BM (patient 1; Supplemental Tables 3 and 5), ^{18}F-FET PET at follow-up 12 wk after treatment initiation (bottom row) shows significant decrease of metabolic activity (TBR_{mean}, −28%) compared with baseline (top row), although MRI changes were consistent with progression according to iRANO criteria. Reduction of metabolic activity was associated with stable clinical course over 10 mo. CE = contrast-enhanced.

DISCUSSION

The main finding of the present study is that ^{18}F-FET PET seems to be of great value for the differentiation of treatment-related changes predominantly induced by

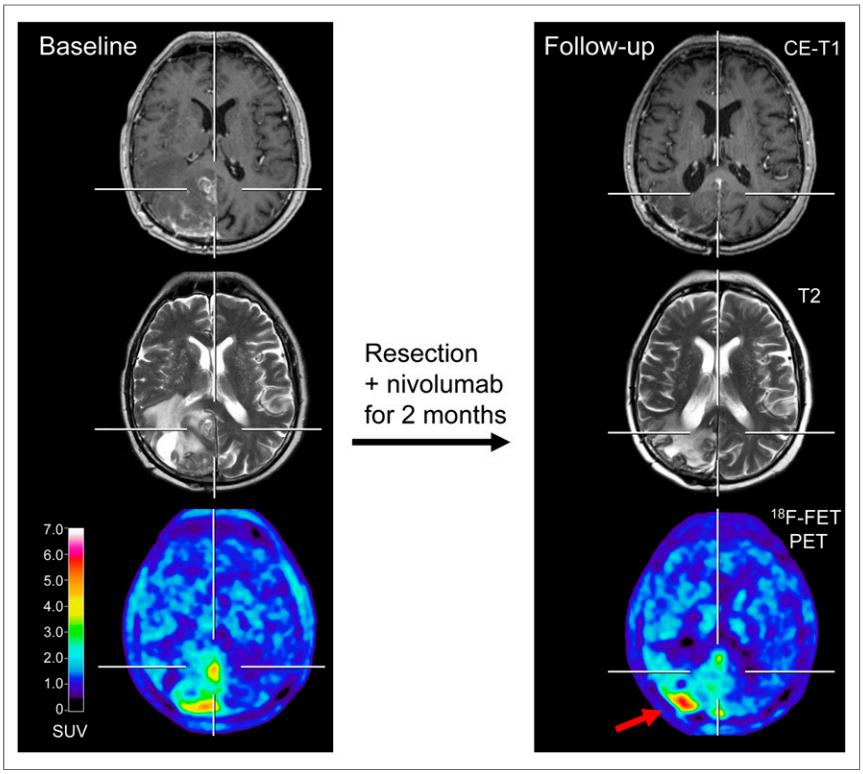

FIGURE 3. A 67-y-old patient with multiple BMs secondary to NSCLC treated with surgery followed by nivolumab (patient 9; Supplemental Tables 3 and 5). ^{18}F-FET PET at follow-up is consisted with mixed response. Besides reduction of metabolic activity in some lesions, right occipital lesion, in particular, shows increasing metabolic activity (TBR_{mean} increase, 10%). In contrast, corresponding MRI suggested partial response according to iRANO criteria. Patient died 2 mo later. CE = contrast-enhanced.

ICI or TT in combination with radiotherapy from BM relapse in patients with MM or NSCLC. The high diagnostic accuracy (85%) could be obtained by a simple and easily applicable approach (i.e., calculation of TBRs), which facilitates implementation in clinical routine. This finding is of eminent interest since the combination of radiotherapy with ICI or TT may substantially increase the risk for treatment-related changes such as radiation necrosis (*10,28–31*). Another important observation in our study is that static and dynamic ^{18}F-FET PET parameters may be helpful for the identification of both responders and nonresponders to a treatment regimen including ICI or TT with a similar high diagnostic performance (range of accuracy, sensitivity, and specificity, 80%–83%). Importantly, metabolic ^{18}F-FET PET responders exhibited a significantly longer stable clinical course during the follow-up than did metabolic nonresponders (median time, 10.5 vs. 4 mo). Moreover, ^{18}F-FET PET provided additional important clinical information for treatment response evaluation beyond the information provided by contrast-enhanced MRI alone, that is, in terms of identification of false-positive or false-negative MRI findings. Since radiotherapy, immunotherapy with ICI, or TT—especially in combination—plays an increasingly important role in personalized treatment of BM, diagnostic information obtained from ^{18}F-FET PET may therefore be of value for patient management. In particular, supplemental ^{18}F-FET PET in cases of ambiguous MRI findings is advantageous for treatment monitoring, providing neurooncologists with a longer time window for subsequent patient management.

Our findings are in line with a small pilot study that highlighted for the first time the potential of ^{18}F-FET PET to identify pseudoprogression in patients with BM originating from MM treated with ICI (*32*). In relation to previous studies evaluating the accuracy of amino acid PET for the diagnosis of treatment-related changes in patients with BM treated solely with radiotherapy (predominantly radiosurgery), our results are also comparable. These studies using various radiolabeled amino acids, including ^{18}F-FET, consistently revealed that the sensitivity and specificity for the differentiation of treatment-related changes from BM relapse is in the range of 80%–90% (*24,33–40*). Additionally, parameters obtained from dynamic ^{18}F-FET PET acquisition seem to further increase the diagnostic performance compared with static parameters alone (*24,34,38*).

However, in the patients of our study treated with ICI or TT plus radiotherapy (i.e., most patients), the dynamic ^{18}F-FET PET parameter TTP was not able to further improve diagnostic accuracy in terms of differentiation between treatment-related changes and BM relapse. Most probably, this finding is related to the relatively low number of patients available for dynamic data evaluation. Conversely, a recent study suggested that the dynamic ^{18}F-FET PET parameter TTP might be helpful for differentiating pseudoprogression from BM relapse in NSCLC patients (n = 11) who underwent radiotherapy in combination with ICI (*41*). In that study, however, both the low number of time frames (range, 5–8 frames) and the long duration of time frames (5 min each) in the applied dynamic PET scanning protocol do not allow a meaningful analysis of ^{18}F-FET uptake over the time, especially in the early phase of dynamic PET acquisition (i.e., 0–20 min after injection).

Notwithstanding, regarding assessment of response to a treatment regimen including ICI or TT, we observed that the change in the dynamic parameter TTP at follow-up PET imaging seems to be of value to identify both metabolic responders and nonresponders. Furthermore, the observed decline in metabolic activity as assessed by TBRs in responding patients (≥10% compared with baseline imaging), which was associated with a significantly longer stable follow-up, is similar to glioblastoma patients who had a metabolic ^{18}F-FET PET response to chemoradiation with temozolomide (*42*).

Taken together, our findings highlight that newer treatment options have requirements on neuroimaging that cannot be met by conventional MRI. Non–amino acid PET tracers also seem to be of value for treatment monitoring of these newer treatment options for patients with BM. For example, the tracer 3′-deoxy-3′-^{18}F-fluorothymidine, an analog of the nucleoside thymidine and a marker for cellular proliferation, was used in BM patients secondary to MM treated with immunotherapy using ICI or TT (*43*). It was observed that responding patients may show a more pronounced proliferative reduction on 3′-deoxy-3′-^{18}F-fluorothymidine PET than the reduction of contrast enhancement on standard MRI.

Nevertheless, the present study had several limitations. Because of its retrospective nature, the findings should be interpreted with caution and warrant confirmation by a prospective study. One might argue that the number of included patients was relatively low. Nevertheless, our dataset included the highest number of patients treated with ICI or TT, predominantly with radiotherapy, who were monitored with ^{18}F-FET PET (in part even with serial scans), allowing a more profound evaluation of this clinically promising imaging technique. Another putative weakness was the heterogeneity of the applied treatment. Apart from clinical trials, this heterogeneity represents a real-life constellation in many brain tumor centers and reflects the current concept of personalized medicine in cancer patients. Furthermore, because multiple lesions frequently occurred and tissue for neuropathologic evaluation obtained by biopsy was not available, radiologic and clinical criteria had to be used for the final diagnosis for most lesions. However, in clinical routine, ethical issues or medical contraindications frequently influence the indication for a biopsy. Since alternative diagnostic methods such as liquid biopsy are clinically not yet established, the assessment of response by radiologic and clinical criteria is a reasonable alternative.

CONCLUSION

Our findings suggest that ^{18}F-FET PET is a useful method in clinically challenging situations, especially when conventional MRI is equivocal. The detection of BM relapse with high accuracy, as well as the reliable assessment of response, is essential for optimizing patient counseling and the treatment concept for each patient. Furthermore, this approach achieves an accuracy that is sufficient to influence clinical decision making and may therefore help to reduce the number of invasive diagnostic interventions and overtreatment for a considerable number of seriously ill patients with BM. A larger prospective study is warranted to confirm the clinical usefulness of ^{18}F-FET PET–derived imaging parameters for treatment monitoring of regimens that include newer treatment options such as ICI or TT.

DISCLOSURE

The Cologne Clinician Scientist-Program (CCSP) of the Deutsche Forschungsgemeinschaft (DFG, FI 773/15-1), Germany, supported this work. No other potential conflict of interest relevant to this article was reported.

KEY POINTS

QUESTION: What is the diagnostic value of ^{18}F-FET PET in patients with BM undergoing IT or TT?

PERTINENT FINDINGS: Amino acid PET using the tracer ^{18}F-FET may add valuable information for the diagnosis of treatment-related changes in BM patients undergoing ICI or TT alone or in combina tion with radiotherapy. ^{18}F-FET PET helps to identify responders to radiotherapy in combination with ICI or TT. Conventional MRI find ings can be discrepant (i.e., unchanged or even progressive) in ^{18}F-FET PET responders. Responding patients on ^{18}F-FET PET had a significantly longer stable clinical course of 6 mo or more

IMPLICATIONS FOR PATIENT CARE: Treatment monitoring using ^{18}F-FET PET achieves an accuracy that is sufficient to influence clinical decision making and may help to reduce the number of invasive diagnostic interventions and overtreatment for a considerable number of seriously ill patients with BM.

REFERENCES

1. Soffietti R, Abacioglu U, Baumert B, et al. Diagnosis and treatment of brain metastases from solid tumors: guidelines from the European Association of Neuro-Oncology (EANO). *Neuro Oncol.* 2017;19:162–174.
2. Reck M, Rodriguez-Abreu D, Robinson AG, et al. Pembrolizumab versus chemotherapy for PD-L1-positive non-small-cell lung cancer. *N Engl J Med.* 2016; 375:1823–1833.
3. Borghaei H, Paz-Ares L, Horn L, et al. Nivolumab versus docetaxel in advanced nonsquamous non-small-cell lung cancer. *N Engl J Med.* 2015;373: 1627–1639.
4. Flaherty KT, Infante JR, Daud A, et al. Combined BRAF and MEK inhibition in melanoma with BRAF V600 mutations. *N Engl J Med.* 2012;367:1694–1703.
5. Long GV, Atkinson V, Lo S, et al. Combination nivolumab and ipilimumab or nivolumab alone in melanoma brain metastases: a multicentre randomised phase 2 study. *Lancet Oncol.* 2018;19:672–681.
6. Wu YL, Ahn MJ, Garassino MC, et al. CNS efficacy of osimertinib in patients with T790M-positive advanced non-small-cell lung cancer: data from a randomized phase III trial (AURA3). *J Clin Oncol.* 2018;36:2702–2709.
7. Tawbi HA, Forsyth PA, Algazi A, et al. Combined nivolumab and ipilimumab in melanoma metastatic to the brain. *N Engl J Med.* 2018;379:722–730.
8. Davies MA, Saiag P, Robert C, et al. Dabrafenib plus trametinib in patients with BRAF(V600)-mutant melanoma brain metastases (COMBI-MB): a multicentre, multicohort, open-label, phase 2 trial. *Lancet Oncol.* 2017;18:863–873.
9. Okada H, Weller M, Huang R, et al. Immunotherapy response assessment in neuro-oncology: a report of the RANO working group. *Lancet Oncol.* 2015;16: e534–e542.
10. Galldiks N, Kocher M, Ceccon G, et al. Imaging challenges of immunotherapy and targeted therapy in patients with brain metastases: response, progression, and pseudoprogression. *Neuro Oncol.* 2020;22:17–30.
11. Cohen JV, Alomari AK, Vortmeyer AO, et al. Melanoma brain metastasis pseudoprogression after pembrolizumab treatment. *Cancer Immunol Res.* 2016;4: 179–182.
12. Langen KJ, Galldiks N, Hattingen E, Shah NJ. Advances in neuro-oncology imaging. *Nat Rev Neurol.* 2017;13:279–289.
13. Okubo S, Zhen HN, Kawai N, Nishiyama Y, Haba R, Tamiya T. Correlation of L-methyl-^{11}C-methionine (MET) uptake with L-type amino acid transporter 1 in human gliomas. *J Neurooncol.* 2010;99:217–225.
14. Youland RS, Kitange GJ, Peterson TE, et al. The role of LAT1 in ^{18}F-DOPA uptake in malignant gliomas. *J Neurooncol.* 2013;111:11–18.
15. Papin-Michault C, Bonnetaud C, Dufour M, et al. Study of LAT1 expression in brain metastases: towards a better understanding of the results of positron emission tomography using amino acid tracers. *PLoS One.* 2016;11:e0157139.
16. Albert NL, Weller M, Suchorska B, et al. Response Assessment in Neuro-Oncology Working Group and European Association for Neuro-Oncology recommendations for the clinical use of PET imaging in gliomas. *Neuro Oncol.* 2016; 18:1199–1208.
17. Galldiks N, Langen KJ, Albert NL, et al. PET imaging in patients with brain metastasis: report of the RANO/PET group. *Neuro Oncol.* 2019;21:585–595.
18. Law I, Albert NL, Arbizu J, et al. Joint EANM/EANO/RANO practice guidelines/SNMMI procedure standards for imaging of gliomas using PET with radiolabelled amino acids and [^{18}F]FDG: version 1.0. *Eur J Nucl Med Mol Imaging.* 2019;46:540–557.
19. Ellingson BM, Bendszus M, Boxerman J, et al. Consensus recommendations for a standardized brain tumor imaging protocol in clinical trials. *Neuro Oncol.* 2015;17:1188–1198.
20. Lin NU, Lee EQ, Aoyama H, et al. Response assessment criteria for brain metastases: proposal from the RANO group. *Lancet Oncol.* 2015;16:e270–e278.
21. Hamacher K, Coenen HH. Efficient routine production of the ^{18}F-labelled amino acid O-2-^{18}F fluoroethyl-L-tyrosine. *Appl Radiat Isot.* 2002;57:853–856.
22. Herzog H, Langen KJ, Weirich C, et al. High resolution BrainPET combined with simultaneous MRI. *Nuklearmedizin.* 2011;50:74–82.
23. Pauleit D, Floeth F, Hamacher K, et al. O-(2-[^{18}F]fluoroethyl)-L-tyrosine PET combined with MRI improves the diagnostic assessment of cerebral gliomas. *Brain.* 2005;128:678–687.
24. Ceccon G, Lohmann P, Stoffels G, et al. Dynamic O-(2-^{18}F-fluoroethyl)-L-tyrosine positron emission tomography differentiates brain metastasis recurrence from radiation injury after radiotherapy. *Neuro-oncol.* 2017;19:281–288.
25. Langen KJ, Bartenstein P, Boecker H, et al. German guidelines for brain tumour imaging by PET and SPECT using labelled amino acids [in German]. *Nucl Med (Stuttg).*2011;50:167–173.
26. Kinahan PE, Fletcher JW. Positron emission tomography-computed tomography standardized uptake values in clinical practice and assessing response to therapy. *Semin Ultrasound CT MR.* 2010;31:496–505.

27. Galldiks N, Stoffels G, Filss C, et al. The use of dynamic *O*-(2-^{18}F-fluoroethyl)-L-tyrosine PET in the diagnosis of patients with progressive and recurrent glioma. *Neuro Oncol.* 2015;17:1293–1300.
28. Kroeze SG, Fritz C, Hoyer M, et al. Toxicity of concurrent stereotactic radiotherapy and targeted therapy or immunotherapy: a systematic review. *Cancer Treat Rev.* 2017;53:25–37.
29. Fang P, Jiang W, Allen P, et al. Radiation necrosis with stereotactic radiosurgery combined with CTLA-4 blockade and PD-1 inhibition for treatment of intracranial disease in metastatic melanoma. *J Neurooncol.* 2017;133:595–602.
30. Trommer-Nestler M, Marnitz S, Kocher M, et al. Robotic stereotactic radiosurgery in melanoma patients with brain metastases under simultaneous anti-PD-1 treatment. *Int J Mol Sci.* 2018;19:2653.
31. Galldiks N, Lohmann P, Werner JM, Ceccon G, Fink GR, Langen KJ. Molecular imaging and advanced MRI findings following immunotherapy in patients with brain tumors. *Expert Rev Anticancer Ther.* 2020;20:9–15.
32. Kebir S, Rauschenbach L, Galldiks N, et al. Dynamic O-(2-[^{18}F]fluoroethyl)-L-tyrosine PET imaging for the detection of checkpoint inhibitor-related pseudoprogression in melanoma brain metastases. *Neuro Oncol.* 2016;18:1462–1464.
33. Terakawa Y, Tsuyuguchi N, Iwai Y, et al. Diagnostic accuracy of ^{11}C-methionine PET for differentiation of recurrent brain tumors from radiation necrosis after radiotherapy. *J Nucl Med.* 2008;49:694–699.
34. Galldiks N, Stoffels G, Filss CP, et al. Role of *O*-(2-^{18}F-fluoroethyl)-L-tyrosine PET for differentiation of local recurrent brain metastasis from radiation necrosis. *J Nucl Med.* 2012;53:1367–1374.
35. Lizarraga KJ, Allen-Auerbach M, Czernin J, et al. ^{18}F-FDOPA PET for differentiating recurrent or progressive brain metastatic tumors from late or delayed radiation injury after radiation treatment. *J Nucl Med.* 2014;55:30–36.
36. Cicone F, Minniti G, Romano A, et al. Accuracy of F-DOPA PET and perfusion-MRI for differentiating radionecrotic from progressive brain metastases after radiosurgery. *Eur J Nucl Med Mol Imaging.* 2015;42:103–111.
37. Minamimoto R, Saginoya T, Kondo C, et al. Differentiation of brain tumor recurrence from post-radiotherapy necrosis with ^{11}C-methionine PET: visual assessment versus quantitative assessment. *PLoS One.* 2015;10: e0132515.
38. Romagna A, Unterrainer M, Schmid-Tannwald C, et al. Suspected recurrence of brain metastases after focused high dose radiotherapy: can [^{18}F]FET-PET overcome diagnostic uncertainties? *Radiat Oncol.* 2016;11:139.
39. Yomo S, Oguchi K. Prospective study of ^{11}C-methionine PET for distinguishing between recurrent brain metastases and radiation necrosis: limitations of diagnostic accuracy and long-term results of salvage treatment. *BMC Cancer.* 2017; 17:713.
40. Lohmann P, Kocher M, Ceccon G, et al. Combined FET PET/MRI radiomics differentiates radiation injury from recurrent brain metastasis. *Neuroimage Clin.* 2018;20:537–542.
41. Akhoundova D, Hiltbrunner S, Mader C, et al. ^{18}F-FET PET for diagnosis of pseudoprogression of brain metastases in patients with non-small cell lung cancer. *Clin Nucl Med.* 2020;45:113–117.
42. Galldiks N, Langen K, Holy R, et al. Assessment of treatment response in patients with glioblastoma using *O*-(2-^{18}F-fluoroethyl)-L-tyrosine PET in comparison to MRI. *J Nucl Med.* 2012;53:1048–1057.
43. Nguyen NC, Yee MK, Tuchayi AM, Kirkwood JM, Tawbi H, Mountz JM. Targeted therapy and immunotherapy response assessment with F-18 fluorothymidine positron-emission tomography/magnetic resonance imaging in melanoma brain metastasis: a pilot study. *Front Oncol.* 2018;8:18.